First Order Reliability Method With Truncated Random Variables

Xiaoping Du[1]
Associate Professor
e-mail: dux@mst.edu

Zhen Hu
Research Assistant
e-mail: zh4hd@mst.edu

Department of Mechanical and Aerospace Engineering,
Missouri University of Science and Technology,
290D Toomey Hall,
400 West 13th Street,
Rolla, MO 65409-0500

In many engineering applications, the probability distributions of some random variables are truncated; these truncated distributions are resulted from restricting the domain of other probability distributions. If the first order reliability method (FORM) is directly used, the truncated random variables will be transformed into unbounded standard normal distributions. This treatment may result in large errors in reliability analysis. In this work, we modify FORM so that the truncated random variables are transformed into truncated standard normal variables. After the first order approximation and variable transformation, saddlepoint approximation is then used to estimate the reliability. Without increasing the computational cost, the proposed method is generally more accurate than the original FORM for problems with truncated random variables. [DOI: 10.1115/1.4007150]

Keywords: reliability, first order reliability method, truncated random variables, saddlepoint approximations

1 Introduction

Truncated random variables are commonly encountered in engineering applications. Their probability distributions are resulted from restricting the domain of other probability distributions. For example, design engineers typically specify tolerances for their design variables, such as the dimension variables that define the geometry of a part. Factories always institute quality controls to meet tolerance specifications [1–3]. If the part dimensions fall outside the tolerance specifications, the part may be scrapped or reworked. If a dimension variable follows a normal distribution, its distribution is then a doubly truncated normal distribution. To ensure high energy efficiency and safety, engineers also specify cut-in and cut-out velocities, at which wind/hydrokinetic turbines will cease power generation and shut down. Hence the wind/river speed used in designing a turbine is also a truncated random variable [4–8]. Similarly, the material strength may also be bounded because defective materials may be screened out before they are put into use [9–12]. The earthquake magnitude is also often modeled as a truncated exponential distribution [13–15]. Truncated random variables are, therefore, involved in various engineering problems.

The most commonly used reliability method, the first order reliability method (FORM) [16–18], can handle any continuous distributions. But the way it handles truncated distributions may produce large errors in the reliability analysis. There is a need to improve the accuracy when truncated random variables exist.

In this work, we restrict our discussions on those truncated distributions that are resulted from restricting the domain of their original probability distributions. The original distributions we consider here are those that are commonly used in FORM, including normal, lognormal, Weibull, Beta, exponential, Gumbel, extreme value type I and II, uniform, and Gamma distributions.

Suppose a response variable Z can be computationally evaluated with a limit-state function given by

$$Z = g(\mathbf{X}, \tilde{\mathbf{Y}}) \tag{1}$$

where $\mathbf{X}$ and $\tilde{\mathbf{Y}}$ are vectors of untruncated random variables and truncated random variables, respectively.

If a failure occurs when $g(\cdot) < 0$, the probability of failure is calculated by

$$p_f = \Pr\{g(\mathbf{X}, \tilde{\mathbf{Y}}) < 0\} \tag{2}$$

where $\Pr\{\cdot\}$ stands for the probability. To calculate this probability, FORM transforms $\mathbf{X} = (X_1, X_2, \ldots, X_n)$ and $\tilde{\mathbf{Y}} = (\tilde{Y}_1, \tilde{Y}_2, \ldots \tilde{Y}_m)$ into independent random variables that follow standard normal distributions. It then searches for a special point, called the most probable point (MPP). Once the MPP is found, the limit-state function is linearized at the MPP, and p_f can be easily obtained [19–24].

When FORM is used, a truncated random variable is transformed into an unbounded random variable because a standard normal random variable varies from $-\infty$ to $+\infty$. This treatment not only causes numerical difficulties but also a loss of accuracy. The reason of numerical difficulties has been studied in Ref. [25]. The study shows that for truncated random variables the MPP search algorithm may completely breakdown, and modifications to the standard iterative FORM algorithm have been proposed. The method, however, does not improve the accuracy of the original FORM when it is used for truncated distributions.

Other studies on truncated random variables have also been reported. Millwater and Feng [26] proposed a sensitivity analysis method with respect to bounds of truncated distributions. Li [2] developed a method of minimizing the expected quality loss of products by optimizing the truncated bounds of manufacturing tolerances. Zhang and Xie [27] investigated the characteristics and application of the truncated Weibull distribution. Raschke [28] constructed an estimator for the right truncation point of a truncated exponential distribution. By using the software package NESSUS, Griffin and Wieland [29] analyzed the reliability of a composite fighter wing with truncated normal random variables,

[1]Corresponding author.

Contributed by the Design Automation Committee of ASME for publication in the Journal of Mechanical Design. Manuscript received December 1, 2011; final manuscript received April 29, 2012; published online August 9, 2012. Assoc. Editor: David Gorsich.

 Copyright © 2012 by ASME

Downloaded From: http://mechanicaldesign.asmedigitalcollection.asme.org/ on 03/21/2013 Terms of Use: http://asme.org/terms

and their results show that the truncated random variables can well present the uncertainties in design variables. Butler and Wood [30] presented two types of representation of moment generating function for a truncated random variable.

The purpose of this work is to improve the accuracy of FORM when truncated random variables exist. The major strategy we implement is to transform the truncated random variables into truncated standard normal variables. Next, we discuss general equations for truncated random variables in Sec. 2 and then briefly review FORM in Sec. 3. The modified FORM is presented in Sec. 4 followed by two numerical examples in Sec. 5. Conclusions are given in Sec. 6.

2 Truncated Random Variables

Let Y_j $(j = 1, 2, \ldots, m)$ be a continuous random variable, and denote its probability density function (PDF) and cumulative distribution function (CDF) as $f_{Y_j}(y)$ and $F_{Y_j}(y)$, respectively. If restricting the domain of Y_j by $a_j \le Y_j \le b_j$, we then have a new random variable, denoted by $\tilde{Y}_j$, and we call it a truncated random variable. We also call Y_j the original variable of $\tilde{Y}_j$.

Denote the PDF and CDF of $\tilde{Y}_j$ by $f_{\tilde{Y}_j}(y)$ and $F_{\tilde{Y}_j}(y)$, respectively. $f_{\tilde{Y}_j}(y)$ is given by

$$f_{\tilde{Y}_j}(y) = p_{Y_j} f_{Y_j}(y) \text{ where } a_j \le y \le b_j \tag{3}$$

where p_{Y_j} is a constant. Integrating the above PDF from a_j to b_j yields 1.0, and therefore

$$p_{Yj} = 1/\left[F_{Y_j}(b_j) - F_{Y_j}(a_j)\right] \tag{4}$$

where $F_{Y_j}(a_j)$ and $F_{Y_j}(b_j)$ are the CDFs of Y_j at a_j and b_j, respectively.

Integrating the PDF, we obtain the CDF of $\tilde{Y}_j$

$$F_{\tilde{Y}_j}(y) = p_{Yj}[F_{Y_j}(y) - F_{Y_j}(a_j)] \text{ where } a_j \le y \le b_j \tag{5}$$

3 First Order Reliability Method (FORM) With Truncated Random Variables

In this section, we explain why the direct use of FORM may produce a large error. We assume that all random variables $(\mathbf{X}, \tilde{\mathbf{Y}})$ are independent, but the results can be extended to dependent variables. FORM involves the following three steps:

(1) Transformation of random variables:

Random variables $(\mathbf{X}, \tilde{\mathbf{Y}})$ are transformed into random variables $\mathbf{U} = (\mathbf{U}_X, \mathbf{U}_Y)$ whose components follow standard normal distributions. The transformation for $\mathbf{X}$ is given by

$$X_i = F_{Xi}^{-1}(\Phi(U_{Xi})) = T(U_{Xi}) \quad (i = 1, 2, \ldots, n) \tag{6}$$

where $\Phi(\cdot)$ and $F_{Xi}(\cdot)$ are the CDFs of U_i and X_i, respectively, $F_{Xi}^{-1}(\cdot)$ is the inverse function of $F_{Xi}(\cdot)$, and $T(\cdot)$ stands for the transformation.

For a truncated variable $\tilde{Y}_j$ $(j = 1, 2, \ldots, m)$, using Eqs. (5) and (6), we have the transformation as follows:

$$\tilde{Y}_j = F_{Y_j}^{-1}\left(\frac{\Phi(U_{\tilde{Y}_j})}{p_{Yj}} + F_{Y_j}(a_j)\right) \tag{7}$$

(2) MPP search:

The most probable point (MPP) $\mathbf{u}^*$ is at the limit state $g(T(\mathbf{U})) = 0$, and at the MPP the joint probability density of $\mathbf{U}$ is maximal. The MPP is obtained by solving

$$\begin{cases} \min\limits_{\mathbf{u}} \|\mathbf{u}\| \\ \text{subject to } g(T(\mathbf{u})) = 0 \end{cases} \tag{8}$$

where $\|\cdot\|$ stands for the magnitude of a vector. The MPP is the shortest distance point from $g(T(\mathbf{U})) = 0$ to the origin. The distance $\beta = \|\mathbf{u}^*\|$ is called the *reliability index*.

(3) Probability calculation:

After the limit-state function is linearized at the MPP, the probability of failure can be easily computed by

$$p_f = \Phi(-\beta) \tag{9}$$

We now use a limit-state function $g(\tilde{\mathbf{Y}}) = 2 - \tilde{Y}_1 - \tilde{Y}_2$, as an example, to show the effect of the direct use of FORM on the accuracy of the analysis result. The two truncated random variables $\tilde{Y}_1$ and $\tilde{Y}_2$ are derived from two independent standard normal variables $Y_1 \sim N(0, 1^2)$ and $Y_2 \sim N(0, 1^2)$, respectively. $\tilde{Y}_1$ and $\tilde{Y}_2$ are doubly truncated with the same interval $[-2, 2]$. Then according to Eq. (5), the CDFs of $\tilde{Y}_1$ and $\tilde{Y}_2$ are given by $F_{\tilde{Y}_j}(y) = p_{Y_j}[\Phi(y) - \Phi(-2)], j = 1, 2$ where $p_{Y_j} = 1/[\Phi(2) - \Phi(-2)]$. The PDFs of $f_{\tilde{Y}_j}(y)$ are $p_{Y_j}\phi(y), j = 1, 2$, where $\phi(\cdot)$ is the PDF of a standard normal distribution.

The probability of failure $p_f = \Pr\{g(\mathbf{Y}) = 2 - \tilde{Y}_1 - \tilde{Y}_2 < 0\}$ can be theoretically obtained by integrating the joint PDF of $\tilde{Y}_1$ and $\tilde{Y}_2$ over the failure region, which is a closed domain determined by $2 - (\tilde{Y}_1 - \tilde{Y}_2) < 0$, $0 < \tilde{Y}_1 < 2$, and $0 < \tilde{Y}_2 < 2$, as shown in Fig. 1. The integral is given by

$$\begin{aligned} p_f &= \iint_{g(\tilde{\mathbf{Y}})<0} f_{\tilde{Y}_1}(y_1) f_{\tilde{Y}_2}(y_2) dy_1 dy_2 \\ &= \int_0^2 \int_{2-y_1}^2 p_{Y_1} p_{Y_2} \phi(y_1)\phi(y_2) dy_1 dy_2 \\ &= p_{Y_1} p_{Y_2} \int_0^2 [\Phi(2) - \Phi(2 - y_1)] dy_1 = 0.0551 \end{aligned} \tag{10}$$

The contour of the limit-state function at $g(\tilde{\mathbf{Y}}) = 0$, the contours of the joint PDF, and the integration (failure) region are also plotted in Fig. 1.

We now use FORM to calculate p_f. We first transform the truncated random variables $\tilde{Y}_j$ into U_{Y_j} by

$$\tilde{Y}_j = \Phi^{-1}\left(\frac{\Phi(U_{Y_j})}{p_{Y_j}} + \Phi(-2)\right) \text{ where } -2 \le \tilde{Y}_j \le 2 \tag{11}$$

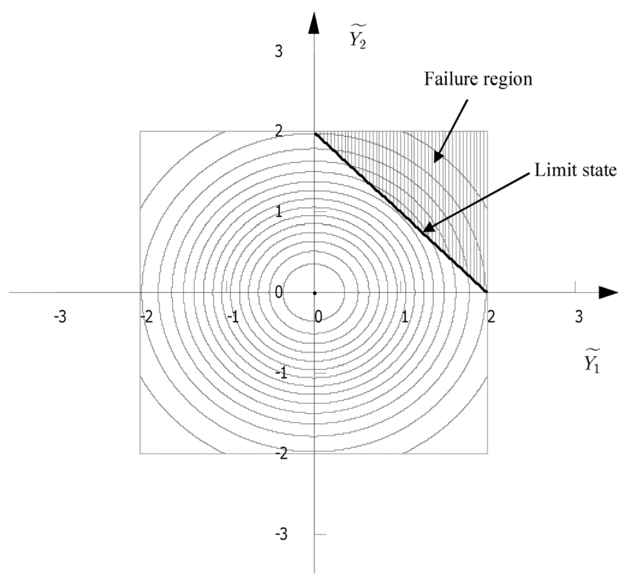

Fig. 1 Failure region and limit-state function in original random space

Downloaded From: http://mechanicaldesign.asmedigitalcollection.asme.org/ on 03/21/2013 Terms of Use: http://asme.org/terms

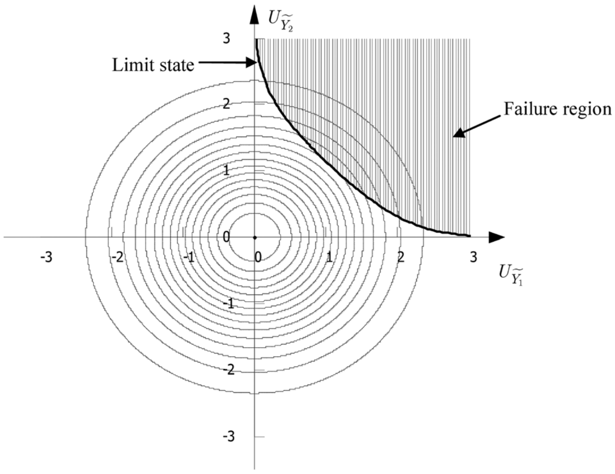

Fig. 2 Failure region and limit-state function in transformed random space

After the transformation, the random variables are U_{Y_j} where $j = 1, 2$, and the linear limit-state function becomes nonlinear because the limit-state function in the U-space is $g(T(\mathbf{U}_{\tilde{Y}}))=2-\{\Phi^{-1}[\Phi(U_{Y_1})/\ p_{Y_1}+\Phi(-2)]+\Phi^{-1}[\Phi(U_{Y_2})/p_{Y_2}+\Phi(-2)]\}$. The reliability index can be easily found to be $\beta = -\sqrt{2}\Phi^{-1}[\Phi(1) - \Phi(-2)/\ (\Phi(2) - \Phi(-2))] = -1.5127$, and the probability of failure is $p_f = \Phi(-\beta) = 0.0652$. Relative to the accurate result 0.0551, the error of FORM is 18.3%. Figure 2 shows the nonlinear limit-state function.

This simple example indicates that the transformation from truncated random variables into unbounded standard normal variables may increase the nonlinearity of a limit-state function. This in turn may magnify the error of FORM because it is based on the first order approximation or linearization.

4 New Method With Truncated Random Variables

To overcome the drawback of the original transformation in FORM, we propose to transform truncated random variables into truncated standard normal variables with the same truncation probabilities. Before deriving equations for the new method, we use the above simple example again to illustrate the advantage of the new transformation method. Doing so will make the transformation less nonlinear. For example, with the new transformation approach, the two truncated variables, $\tilde{Y}_1$ and $\tilde{Y}_2$ in the above example, are transformed into truncated standard normal variables $\tilde{U}_{Y_1}$ and $\tilde{U}_{Y_2}$, which are obtained from two standard normal variables within the interval $[-2, 2]$. This interval corresponds to the same truncation probabilities of $\tilde{Y}_1$ and $\tilde{Y}_2$. Since $\tilde{Y}_1$ and $\tilde{Y}_2$ are also from two standard normal variables, for this special problem, they happen to remain unchanged after the new transformation. Therefore, $\tilde{U}_{Y_1} = \tilde{Y}_1$ and $\tilde{U}_{Y_2} = \tilde{Y}_2$. As a result, the associated limit-state function is untouched, and there is no reason to worry about the increased nonlinearity.

4.1 Transformation of Random Variables. We now discuss how to transform truncated variables $\tilde{\mathbf{Y}}$ into normal variables $\mathbf{U}_Y = (\tilde{U}_{Y1}, \tilde{U}_{Y2}, \ldots \tilde{U}_{Ym})$ that are truncated from the standard normal variables $\mathbf{U} = (U_1, U_2, \ldots, U_m)$. For brevity, we use $\tilde{Y}$ for a general truncated variable $\tilde{Y}_j$ where $j = 1, 2, \ldots, m$ and $\tilde{U}$ for its corresponding truncated standard normal variable, which is a general component in $\tilde{\mathbf{U}}_\mathbf{Y} = (\tilde{U}_{Y_1}, \tilde{U}_{Y_2}, \ldots \tilde{U}_{Y_m})$. We also use U_Y for the original standard normal variable that corresponds to $\tilde{U}$. Our task now is to transform $\tilde{Y}$ into $\tilde{U}_Y$. Suppose the left and right truncation points of $\tilde{Y}$ are a and b, respectively. Also suppose the left and right truncation points of $\tilde{U}_Y$ are u_a and u_b, respectively. The CDF of $\tilde{U}_Y$ is then given by

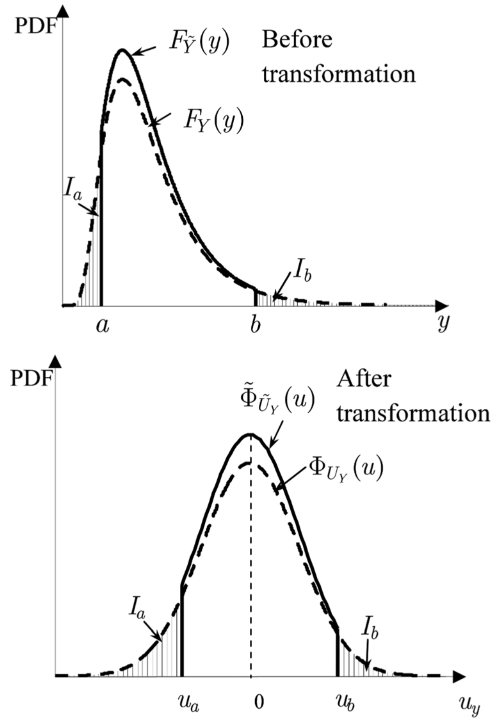

Fig. 3 Transformation of truncated random variables

$$\tilde{\Phi}_{\tilde{U}_Y}(u) = p_U[\Phi(u) - \Phi(u_a)] \text{ where } u_a \le u \le u_b \tag{12}$$

where

$$p_U = 1/[\Phi(u_b) - \Phi(u_a)] \tag{13}$$

And the PDF of $\tilde{U}_Y$ is given by

$$\tilde{\phi}_{\tilde{U}_Y}(u) = p_U\phi(u) \text{ where } u_a \le u \le u_b \tag{14}$$

There are two conditions for the new transformation. The first condition is that the truncation probabilities before and after the transformation are the same. Then the left truncation point u_a of $\tilde{U}_Y$ is determined by

$$I_a = \int_{-\infty}^{a} f_Y(y)dy = \int_{-\infty}^{u_a} \phi(u)du \tag{15}$$

or

$$F_Y(a) = \Phi(u_a) \tag{16}$$

where $f_Y(\cdot)$ and $F_Y(\cdot)$ are the PDF and CDF of Y, respectively, and Y is the original random variable of $\tilde{Y}$.

Similarly, the right truncated point u_b of $\tilde{U}_Y$ is determined by

$$I_b = \int_{b}^{\infty} f_Y(y)dy = \int_{b}^{\infty} \phi(u)du \tag{17}$$

or

$$1 - F_Y(b) = 1 - \Phi(u_b) \tag{18}$$

As shown in Fig. 3, the shaded areas of the two PDF curves truncated out are equal.

The second condition of the transformation is that the CDFs before and after transformation should be the same. This gives

Downloaded From: http://mechanicaldesign.asmedigitalcollection.asme.org/ on 03/21/2013 Terms of Use: http://asme.org/terms

$$F_{\tilde{Y}}(\tilde{Y}) = \tilde{\Phi}_{\tilde{U}_Y}(\tilde{U}_Y) \tag{19}$$

or

$$p_Y[F_Y(\tilde{Y}) - F_Y(a)] = p_U[\Phi(\tilde{U}_Y) - \Phi(u_a)] \tag{20}$$

where $p_Y = 1/[F_Y(b) - F_Y(a)]$ as given in Eq. (4).

With Eqs. (16) and (18),

$$\Phi_{U_Y}(u_b) - \Phi_{U_Y}(u_a) = F_Y(b) - F_Y(a) \tag{21}$$

Therefore, we have $p_Y = p_U$.

Since $F_Y(a) = \Phi(u_a)$ as shown in Eq. (16), Eq. (20) becomes

$$F_Y(\tilde{Y}) = \Phi_{U_Y}(\tilde{U}_Y) \tag{22}$$

or

$$\tilde{Y} = F_Y^{-1}(\Phi_{U_Y}(\tilde{U}_Y)) \tag{23}$$

This new transformation involves only the CDFs of the original random variable Y and the untruncated standard normal variable U. In other words, the transformation for truncated variables from $\tilde{Y}_j$ $(j = 1, 2, \ldots, m)$ to $\tilde{U}_{Y_j}$ is equivalent to the transformation for untruncated variables from Y_j to U_{Y_j}. We can therefore perform the transformation as if the random variables were not truncated. There are two major advantages of this equivalency. As we have already seen in the above simple example, the first advantage is that the new transformation will be less nonlinear than the transformation used in FORM, which is rewritten from Eq. (7) as follows:

$$\tilde{Y} = F_{\tilde{Y}}^{-1}\left(\frac{\Phi(\tilde{U}_Y)}{p_Y} + F_Y(a)\right) \tag{24}$$

We now show the effects of the two transformations for several common distributions, including normal, lognormal, and exponential, in Figs. 4 and 5, and 6, respectively. To quantify the nonlinearity of the transformations, we use the nonlinearity measure proposed in Ref. [31]. We first generated samples for each of the two transformation curves and then used them to fit a straight line. Suppose a transformation is expressed by $Y(U)$ and the corresponding straight line is $L(U)$. The nonlinearity of $Y(U)$ is measured by the square root of the integral of squares of the differences between $Y(U)$ and $L(U)$. The sum of squares is normalized within the range $[U_L, U_U]$ of U. The equation of this nonlinearity measure (NL) is given by Ref. [31]

$$NL = \sqrt{\frac{1}{(U_U - U_L)}\int_{U_L}^{U_U} [Y(U) - L(U)]^2 dU} \tag{25}$$

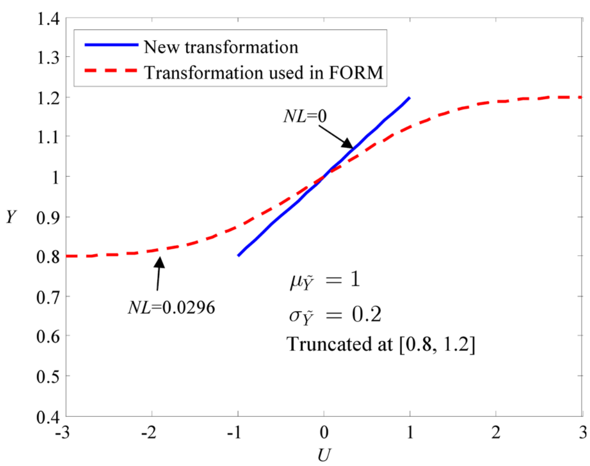

Fig. 4 Transformation of truncated normal distribution

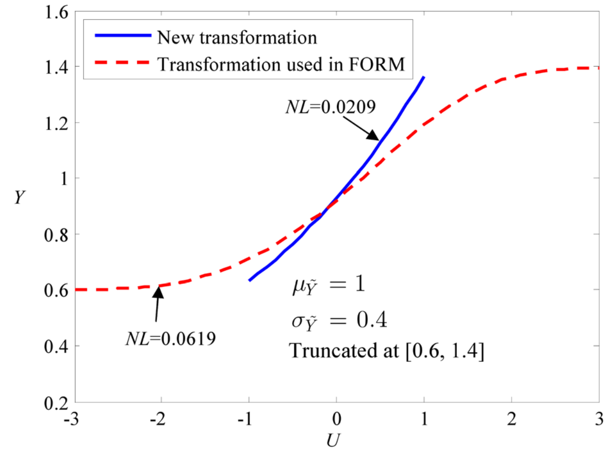

Fig. 5 Transformation of truncated lognormal distribution

In the three examples, the truncated variables are restricted over $[-1, 1]$ in the U-space. Hence $U_L = -1$ and $U_U = 1$ for the new transformation. For the original transformation in FORM, because the range of U is unbounded, we set $U_L = -3$ and $U_U = 3$.

The larger the NL value, the higher is the nonlinearity. If $NL = 0$, the transformation is completely linear. The results in these figures show that the new transformation always produces a smaller NL than the transformation used in FORM. This indicated that the new transformation is less nonlinear than the original transformation.

The other advantage of the new transformation is that the MPP search will not be modified. The reason is that only the CDFs of the original random variables are involved. Then the new transformation is equivalent to transforming the original ransom variables into unbounded standard normal variables. We can, therefore, perform the MPP search with the original random variables and the unbounded standard normal variables. This allows us to use any MPP search algorithms for the original FORM.

4.2 MPP Search. As discussed above, we can use an existing MPP search algorithm for $Z = g(\mathbf{X}, \tilde{\mathbf{Y}})$. After the transformation, the limit-state function becomes

$$Z = g(T(\mathbf{U_X}), T(\tilde{\mathbf{U}}_\mathbf{Y})) \tag{26}$$

where the transformation $T(\cdot)$ for $\mathbf{X}$ is given in Eq. (6), and the transformation $T(\cdot)$ for $\tilde{\mathbf{Y}}$ is given in Eq. (23). The model of the MPP search is then

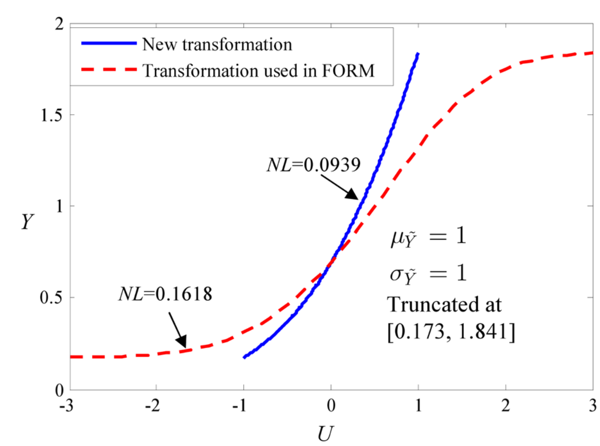

Fig. 6 Transformation of truncated exponential distribution

Downloaded From: http://mechanicaldesign.asmedigitalcollection.asme.org/ on 03/21/2013 Terms of Use: http://asme.org/terms

$$\begin{cases} \min\limits_{(\mathbf{u_X},\tilde{\mathbf{u}}_\mathbf{Y})} \|(\mathbf{u}_X, \tilde{\mathbf{u}}_Y)\| \\ \text{subject to } g(T(\mathbf{u}_X), T(\tilde{\mathbf{u}}_Y)) = 0 \end{cases} \tag{27}$$

The above model is the same as that in Eq. (8). Therefore, any existing MPP search algorithms can be used to solve for the MPP.

4.3 Linearization of the Limit-State Function. After the MPP is found at $\mathbf{u}^* = (\mathbf{u}_X^*, \tilde{\mathbf{u}}_Y^*)$, we linearize the limit-state function at $\mathbf{u}^*$, and this yields

$$Z \approx g(\mathbf{u}_X^*, \tilde{\mathbf{u}}_Y^*) + \sum_{i=1}^{n} \frac{\partial g}{\partial U_{X_i}} (U_{X_i} - u_{X_i}^*) + \sum_{j=1}^{m} \frac{\partial g}{\partial \tilde{U}_{Y_j}} (\tilde{U}_{Y_j} - \tilde{u}_{Y_j}^*) \tag{28}$$

where all the derivatives are those at $\mathbf{u}^*$.

At the MPP $g(\cdot) = 0$, and the limit-state function becomes

$$Z \approx \sum_{i=1}^{n} \frac{\partial g}{\partial U_{X_i}} (U_{X_i} - u_{X_i}^*) + \sum_{j=1}^{m} \frac{\partial g}{\partial \tilde{U}_{Y_j}} (\tilde{U}_{Y_j} - \tilde{u}_{Y_j}^*) \tag{29}$$

Dividing both sides by

$$H = \sqrt{\sum_{i=1}^{n} \left(\frac{\partial g}{\partial U_{X_i}}\right)^2 + \sum_{j=1}^{m} \left(\frac{\partial g}{\partial \tilde{U}_{Y_j}}\right)^2}$$

yields a new limit-state function

$$Z_e(\mathbf{U}_X, \tilde{\mathbf{U}}_Y) = \gamma_0 + \sum_{i=1}^{n} \gamma_{X_i} U_{X_i} + \sum_{j=1}^{m} \gamma_{\tilde{Y}_j} \tilde{U}_{Y_j} \tag{30}$$

where

$$\gamma_0 = -\frac{1}{H} \left[\sum_{i=1}^{n} \frac{\partial g}{\partial U_{X_i}} u_{X_i}^* + \sum_{j=1}^{m} \frac{\partial g}{\partial \tilde{U}_{Y_j}} \tilde{u}_{Y_j}^* \right] \tag{31}$$

$$\gamma_{X_i} = \frac{1}{H} \frac{\partial g}{\partial U_{X_i}} \tag{32}$$

$$\gamma_{\tilde{Y}_j} = \frac{1}{H} \frac{\partial g}{\partial \tilde{U}_{Y_j}} \tag{33}$$

The above three equations can be rewritten as

$$\gamma_0 = \left\| \mathbf{u}_X^*, \tilde{\mathbf{u}}_Y^* \right\| \tag{34}$$

$$\gamma_{X_i} = -\frac{u_{X_i}^*}{\left\| \mathbf{u}_X^*, \tilde{\mathbf{u}}_Y^* \right\|} \tag{35}$$

$$\gamma_{\tilde{Y}_j} = -\frac{\tilde{u}_{Y_j}^*}{\left\| \mathbf{u}_X^*, \tilde{\mathbf{u}}_Y^* \right\|} \tag{36}$$

The new limit-state function is now a linear combination of standard normal random variables $\mathbf{U}_X$ and truncated standard normal variables $\tilde{\mathbf{U}}_Y$. Due to the truncated variables $\mathbf{U}_Y$, unlike the original FORM, the response Z_e will no longer be normally distributed. We need to find a new way to evaluate the probability of failure. Our approach is to use the Saddlepoint approximation.

4.4 Saddlepoint Approximation Based FORM. Saddlepoint approximation can accurately evaluate a CDF especially in a tail area of a distribution [32–37]. The basic requirement of using this approach is to know the cumulative generating function (CGF) of the equivalent limit-state function Z_e in Eq. (30). In this section, we first derive the CGF of Z_e and then apply the saddlepoint approximation.

Suppose the CGF of U_{X_i} is $K_{U_{X_i}}(t)$ and that of $\tilde{U}_{Y_j}$ is $K_{\tilde{U}_{Y_j}}(t)$. Then the CGF of Z_e is

$$K_Z(t) = \gamma_0 t + \sum_{i=1}^{n} K_{U_{Xi}}(\gamma_{X_i} t) + \sum_{j=1}^{m} K_{\tilde{U}_{Yj}}(\gamma_{\tilde{Y}_j} t) \tag{37}$$

For a standard normal random variables U_{X_i}, its CGF and associated derivatives are given by

$$K_{U_{Xi}}(t) = \frac{1}{2} t^2 \tag{38}$$

$$K'_{U_{Xi}}(t) = t \tag{39}$$

$$K''_{U_{Xi}}(t) = 1 \tag{40}$$

Now we derive the CGFs of the truncated variable $\tilde{U}_{Y_j}$. In order to calculate the CGF of $\tilde{U}_{Y_j}$, we first derive its moment generating function (MGF) as follows

$$\begin{aligned} M_{\tilde{U}_{Y_j}}(t) &= \int_{-\infty}^{\infty} \exp(tu) \tilde{\phi}_{\tilde{U}_{Y_j}}(u) du = p_{u_j} \int_{u_{a_j}}^{u_{b_j}} \exp(tu) \phi(u) du \\ &= \frac{p_{u_j}}{\sqrt{2\pi}} \int_{u_{a_j}}^{u_{b_j}} \exp\left\{-\frac{1}{2}(u^2 - 2tu)\right\} du \\ &= \frac{p_{u_j}}{\sqrt{2\pi}} \exp\left(\frac{1}{2}t^2\right) \int_{u_{a_j}-t}^{u_{b_j}-t} \exp\left\{-\frac{1}{2}u^2\right\} du \\ &= p_{u_j} \exp\left(\frac{1}{2}t^2\right) \left\{\Phi(u_{b_j} - t) - \Phi(u_{a_j} - t)\right\} \end{aligned} \tag{41}$$

The CGF of $\tilde{U}_{Y_j}$ and its derivatives are then given by

$$\begin{aligned} K_{\tilde{U}_{Yj}}(t) &= \log M_{\tilde{U}_{Yj}}(t) \\ &= \log p_{u_j} + \frac{1}{2}t^2 + \log\left\{\Phi(u_{b_j} - t) - \Phi(u_{a_j} - t)\right\} \end{aligned} \tag{42}$$

$$K'_{\tilde{U}_{Yj}}(t) = t - \frac{\phi(u_{b_j} - t) - \phi(u_{a_j} - t)}{\Phi(u_{b_j} - t) - \Phi(u_{a_j} - t)} \tag{43}$$

$$\begin{aligned} K''_{\tilde{U}_{Yj}}(t) = 1 &- \frac{\left[\phi(u_{b_j} - t) - \phi(u_{a_j} - t)\right]^2}{\left[\Phi(u_{b_j} - t) - \Phi(u_{a_j} - t)\right]^2} \\ &- \frac{(u_{b_j} - t)\phi(u_{b_j} - t) - (u_{a_j} - t)\phi(u_{a_j} - t)}{\Phi(u_{b_j} - t) - \Phi(u_{a_j} - t)} \end{aligned} \tag{44}$$

Combining Eqs. (36), (37) and (41), we obtain the CGF of Z_e as follows:

$$\begin{aligned} K_Z(t) = \gamma_0 t + \frac{1}{2}\sum_{i=1}^{n} (\gamma_{X_i} t)^2 + \sum_{j=1}^{m} \Bigg\{ & \log p_{u_j} + \frac{1}{2}(\gamma_{\tilde{Y}_j} t)^2 \\ & + \log\left\{\Phi(u_{b_j} - \gamma_{\tilde{Y}_j} t) - \Phi(u_{a_j} - \gamma_{\tilde{Y}_j} t)\right\} \Bigg\} \end{aligned} \tag{45}$$

And the derivatives of $K_Z(t)$ can be obtained using the following equations

$$K'_Z(t) = \gamma_0 + \sum_{i=1}^{n} \gamma_{X_i} K'_{U_{Xi}}(\gamma_{X_i} t) + \sum_{j=1}^{m} \gamma_{\tilde{Y}_j} K'_{\tilde{U}_{Yj}}(\gamma_{\tilde{Y}_j} t) \tag{46}$$

and

$$K''_Z(t) = \sum_{i=1}^{n} \gamma_{X_i}^2 K''_{U_{Xi}}(\gamma_{X_i} t) + \sum_{j=1}^{m} \gamma_{\tilde{Y}_j}^2 K''_{\tilde{U}_{Yj}}(\gamma_{\tilde{Y}_j} t) \tag{47}$$

Downloaded From: http://mechanicaldesign.asmedigitalcollection.asme.org/ on 03/21/2013 Terms of Use: http://asme.org/terms

Substituting Eqs. (39), (40), (43) and (44) into Eqs. (46) and (47), we have

$$K_Z'(t) = \gamma_0 + \sum_{i=1}^{n} \gamma_{X_i}^2 t + \sum_{j=1}^{m} \gamma_{\tilde{Y}_j} \left(\gamma_{\tilde{Y}_j} t - \frac{\phi(u_{b_j} - \gamma_{\tilde{Y}_j} t) - \phi(u_{a_j} - \gamma_{\tilde{Y}_j} t)}{\Phi(u_{b_j} - \gamma_{\tilde{Y}_j} t) - \Phi(u_{a_j} - \gamma_{\tilde{Y}_j} t)} \right) \tag{48}$$

$$K_Z''(t) = \sum_{i=1}^{n} \gamma_{X_i}^2 + \sum_{j=1}^{m} \gamma_{\tilde{Y}_j}^2 \left\{ 1 - \frac{\left[\phi(u_{b_j} - \gamma_{\tilde{Y}_j} t) - \phi(u_{a_j} - \gamma_{\tilde{Y}_j} t)\right]^2}{\left[\Phi(u_{b_j} - \gamma_{\tilde{Y}_j} t) - \Phi(u_{a_j} - \gamma_{\tilde{Y}_j} t)\right]^2} \right\} - \sum_{j=1}^{m} \gamma_{\tilde{Y}_j}^2 \left\{ \frac{(u_{b_j} - \gamma_{\tilde{Y}_j} t)\phi(u_{b_j} - \gamma_{\tilde{Y}_j} t) - (u_{a_j} - \gamma_{\tilde{Y}_j} t)\phi(u_{a_j} - \gamma_{\tilde{Y}_j} t)}{\Phi(u_{b_j} - \gamma_{\tilde{Y}_j} t) - \Phi(u_{a_j} - \gamma_{\tilde{Y}_j} t)} \right\} \tag{49}$$

Although the theory of saddlepoint approximation is complex, its use is straightforward [38–41]. The approximation to the CDF of Z_e derived by Lugananni and Rice [42] is

$$F_{Z_e} = P\{Z_e \le z\} = \Phi(w) + \phi(w)\left(\frac{1}{w} - \frac{1}{v}\right) \tag{50}$$

where

$$w = \text{sign}(t)\{2[t_s z - K_Z(t_s)]\}^{1/2} \tag{51}$$

$$v = t_s\{K_Z''(t_s)\}^{1/2} \tag{52}$$

in which $\text{sign}(t_s) = +1, -1$, or 0, depending on where t_s is positive, negative, or zero. t_s is the saddlepoint and is obtained by solving

$$K_Z'(t) = z \tag{53}$$

As a failure occurs when $z_e < 0$, to obtain p_f, we set $z = 0$ in Eq. (53).

The new method is generally more accurate than FORM. As discussed previously, when FORM is directly used for truncated random variables, its variable transformation may increase the nonlinearity of a limit-state function. The new method can overcome such a drawback. The other advantage of the new method is that any existing MPP search algorithms can be used because the transformation of the new method is equivalent to the variable transformation on only the original variables of the truncated variables. As a result, the efficiency can be maintained as the same as the direct use of FORM. Next we summarize the procedure of the new method.

4.5 Numerical Procedure. We now summarize the procedure of the proposed method with the following steps:

(1) Variable transformation: Obtain the truncation points using Eqs. (16) and (18), transform the regular random variables $\mathbf{X}$ and truncated random variables $\tilde{\mathbf{Y}}$ into standard normal random variables $\mathbf{U}_\mathbf{X}$ and truncated standard normal variables $\tilde{\mathbf{U}}_\mathbf{Y}$ using Eqs. (6) and (23), respectively.
(2) MPP search: Search the MPP using Eq. (27) and obtain the coefficients γ_0, γ_{X_i} and $\gamma_{\tilde{Y}_j}$ by applying Eqs. (34) through (36).
(3) Saddlepoint approximation: Solving for the probability of failure with truncated random variables using Eqs. (50) through (53).

Figure 7 shows the flow chart of the numerical procedure.

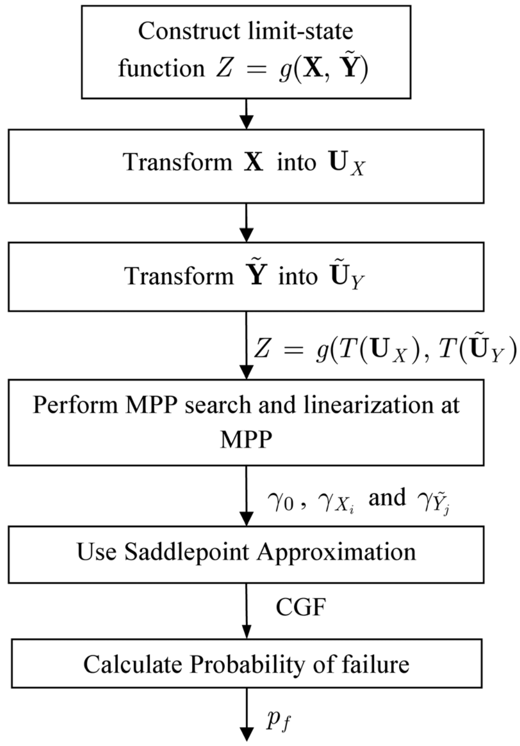

Fig. 7 Flow chart of the numerical procedure

5 Example

In this section, we use two examples to demonstrate the proposed methodology. The first one is for the analysis of a hydrokinetic turbine blade, and the second one is for the analysis of a cantilever beam. The truncation points are nonsymmetric in the first example, and those of the second example are symmetric.

5.1 Example: Hydrokinetic Turbine Analysis. A hydrokinetic turbine blade is shown in Fig. 8. According to the classical

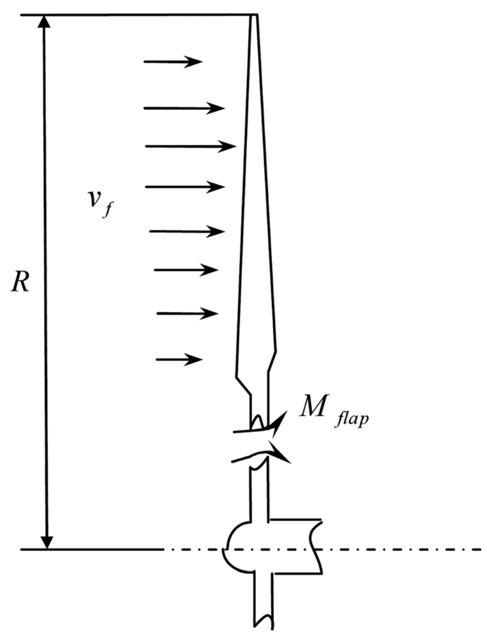

Fig. 8 River flow loading on a hydrokinetic turbine blade

Downloaded From: http://mechanicaldesign.asmedigitalcollection.asme.org/ on 03/21/2013 Terms of Use: http://asme.org/terms

Table 1 Random variables of hydrokinetic turbine blade

Random variable	Mean value	Standard deviation	Distribution type	Truncation point
v_{ext} (m/s)	2.5	0.3	EVT I	[0.7, 4.8]
l_1 (m)	0.21	2.1×10^{-3}	Normal	[0.2037, 0.2163]
t_1 (m)	0.025	2.5×10^{-4}	Normal	[0.0243, 0.0258]
t_2 (m)	0.023	2.3×10^{-4}	Normal	[0.0223, 0.0237]
ε_{allow}	0.02	2×10^{-4}	Normal	[0.0196, 0.0204]

blade element momentum theory, with a fixed tip speed ratio, the flapwise bending moment M_{flap} of the turbine blade is given by

$$M_{flap} = \frac{1}{2}\rho v_{ext}^2 C_m$$

where v_{ext} is the extreme river flow velocity, $\rho = 1\times10^3\,\mathrm{kg/m^3}$ is the river flow density, and $C_m = 0.3522$ is a geometry related coefficient.

The moment of inertia at the root of the blade is

$$I = \frac{1}{12}l_1\left[(2t_1)^3 - (2t_2)^3\right] = \frac{2}{3}l_1(t_1^3 - t_2^3)$$

where l_1, t_1, and t_2 are dimension variables.

Then, the strain ε at the root of the turbine blade is

$$\varepsilon = \frac{M_{flap}y}{EI}$$

where $E = 14$ GPa is the Young's modulus. The maximum strain occurs at $y = t_1$.

The limit-state function is defined by

$$g = \varepsilon_{allow} - \varepsilon$$

where ε_{allow} is the allowable strain of the turbine blade material.

There are five truncated random variables involved in this problem. The river flow velocity is truncated at the cut-in and cut-out velocities, the dimensional random variables are truncated at a 3-σ level, and the allowable strain is truncated at a 2-σ level. The random variables are given in Table 1, where EVT I stands for an Extreme Value Type I distribution, and the distribution parameters are those of the original random variables.

Following the steps in Sec. 4.5, we calculated the probability of failure using the original FORM, the modified FORM, and Monte Carlo simulation (MCS). The MCS result is regarded as an accurate solution because a large sample size of 10^7 was used. The error of the other two methods relative to MCS is computed by

$$\varepsilon = \frac{\left|p_f - p_f^{MCS}\right|}{p_f^{MCS}} \times 100\%$$

where p_f is the probability of failure obtained from either the original FORM or the modified FORM, and p_f^{MCS} is the probability of failure from MCS.

Table 2 Results of reliability analysis of hydrokinetic turbine blades

	O-FORM	M-FORM	MCS
p_f ($\times10^{-6}$)	10.352	6.6123	7.10
N	377	373	1×10^7
Error	45.8%	6.9%	N/A

As shown in Table 2, the accuracy of the modified FORM (M-FORM) is much higher than that of the original FORM (O-FORM) while the computational cost, measured by the number function calls N, is in the same order of magnitude. The result indicates that the proposed method effectively improves the accuracy of FORM with the same level of efficiency when truncated random variables exist.

5.2 Example: Cantilever Beam Analysis. A cantilever beam is shown in Fig. 9 [35]. It is subject to forces F_1 and F_2, moments M_1 and M_2, and distributed loads (q_{L1}, q_{R1}) and (q_{L2}, q_{R2}).

A failure occurs if the deflection at the tip η exceeds the allowable deflection η_{allow}, and the limit-state function is defined by

$$g = \eta_{allow} - \eta$$

where the deflection at the tip is

$$\eta = \frac{1}{EI}\left[\frac{ML^2}{2} + \frac{RL^3}{6} + \sum_{i=1}^{2}\frac{M_i(L-a_i)^2}{2} - \sum_{i=1}^{2}\frac{F_i(L-b_i)^3}{6}\right] - \frac{1}{EI}\left[\sum_{i=1}^{2}\frac{q_{Li}(L-c_i)^4}{24} - \sum_{i=1}^{2}\frac{(q_{Ri}-q_{Li})(L-c_i)^5}{120}\right] + \frac{1}{EI}\left[\sum_{i=1}^{2}\frac{q_{Ri}(L-d_i)^4}{24} + \sum_{i=1}^{2}\frac{(q_{Ri}-q_{Li})(L-d_i)^5}{120}\right]$$

in which the Young's modulus is $E = 200\times10^9$ Pa, and the moment of inertia is $I = (1/12)ph^3$, and the bending moment at root is given by

$$M = -\sum_{i=1}^{2}M_i - \sum_{i=1}^{2}F_ib_i - \sum_{i=1}^{2}q_{Li}(d_i - c_i)(d_i + c_i)/2 - \sum_{i=1}^{2}[(q_{Ri} - q_{Li})(d_i - c_i)/2][(c_i + 2(d_i - c_i)/3)]$$

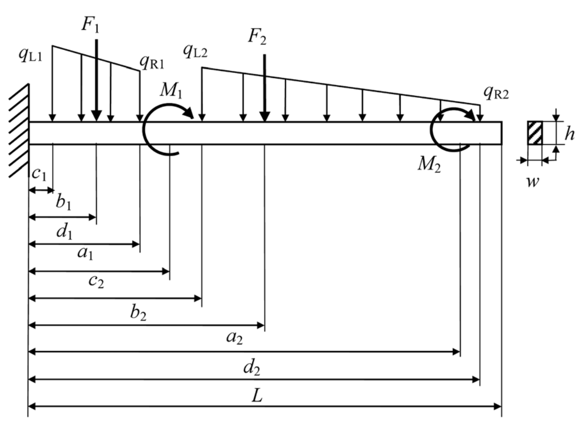

Fig. 9 Cantilever beam

Downloaded From: http://mechanicaldesign.asmedigitalcollection.asme.org/ on 03/21/2013 Terms of Use: http://asme.org/terms

Table 3 Random variables of the cantilever beam

Random variable	Mean value	Standard deviation	Distribution type	Truncation level
M_1 (N·m)	70.0×10^3	7.0×10^3	Normal	k
M_2 (N·m)	50.0×10^3	5.0×10^3	Normal	k
F_1 (N)	20.0×10^3	2.0×10^3	EVT I	k
F_2 (N)	10.0×10^3	1.0×10^3	Normal	k
q_{L1} (N/m)	30.0×10^3	1.0×10^3	Normal	k
q_{R1} (N/m)	20.0×10^3	1.0×10^3	Normal	k
q_{L2} (N/m)	20.0×10^3	1.0×10^3	Normal	k
q_{R2} (N/m)	1.0×10^3	10.0	Normal	k
a_1 (m)	1.5	0.005	Normal	3
a_2 (m)	4.5	0.005	Normal	3
b_1 (m)	0.75	0.001	Normal	3
b_2 (m)	2.50	0.001	Normal	3
c_1 (m)	0.25	0.0005	Normal	3
c_2 (m)	1.75	0.001	Normal	3
d_1 (m)	1.25	0.001	Normal	3
d_2 (m)	4.75	0.001	Normal	3
L (m)	5.0	0.01	Normal	3
w (m)	0.2	0.0001	Normal	3
h (m)	0.4	0.0001	Normal	3
v (m)	9.75×10^{-3}	1.4434×10^{-4}	Normal	3

Table 4 Results of the cantilever example

Truncation level	Result	O-FORM	M-FORM	MCS
$k=5$	p_f ($\times10^{-4}$)	2.3173	2.2554	2.2263
	N	466	424	10^7
	Error	2.4%	0.3%	-
$k=4$	p_f ($\times10^{-4}$)	2.3047	2.1549	2.17
	N	468	424	10^7
	Error	6.2%	0.7%	-
$k=3$	p_f ($\times10^{-4}$)	1.8769	1.2284	1.246
	N	508	424	10^7
	Error	50.6%	1.4%	-
$k=2.5$	p_f ($\times10^{-5}$)	9.9621	4.2073	4.02
	N	618	424	10^7
	Error	147.8%	4.7%	-
$k=2$	p_f ($\times10^{-6}$)	14.272	2.7836	2.85
	N	1000	424	10^8
	Error	400.8%	2.3%	-

Twenty random variables are involved. All of the dimensional random variables are doubly truncated at 3-σ level, and the other random variables are doubly truncated at k-σ level. The distributions of the random variables are given in Table 3.

The reliability analysis results are given in Table 4. The proposed method is again more accurate than the original FORM. The result also shows that the higher is the truncation level or the smaller is the k value, the less accurate is the original FORM. From the numbers of function calls N, we see that both of the FORM methods are equally efficient.

6 Conclusions

The first order reliability method (FORM) has been modified in this work to accommodate truncated random variables. The major modification is to transform truncated random variables into truncated standard normal variables. The transformation allows the new method to use any existing MPP search algorithms. As a result, this treatment can avoid numerical difficulties of the MPP search for truncated variables. Since the linearized limit-state function is not normally distributed with the truncated random variables, using the reliability index to directly calculate the probability of failure is no longer feasible. The other major modification is, therefore, the employment of the saddlepoint approximation.

With the two major modifications, the accuracy of the modified FORM is in general higher than that of the original FORM. Since the MPP search is performed in the same manner as the original FORM, the efficiency of the modified FORM is in the same order of magnitude as the original FORM. As an accurate reliability evaluation method is the basis for reliability-based design (RBD), it is desirable to replace the original FORM with the modified FORM during RBD with truncated random variables.

As the saddlepoint approximation is very accurate in estimating the probability of failure for the linearized limit-state function, the major error of the modified FORM is from the linearization of the limit-state function. This is the intrinsic drawback of FORM. Hence the modified FORM may not be accurate if the limit-state function is highly nonlinear. For this case, one may consider using the second order reliability method (SORM). How to modify SORM for truncated random variables needs a further investigation.

Acknowledgment

The authors gratefully acknowledge the support from the Office of Naval Research through contract ONR N000141010923 (Program Manager – Dr. Michele Anderson) and the Intelligent Systems Center at the Missouri University of Science and Technology.

References

[1] Pearn, W. L., Hung, H. N., Peng, N. F., and Huang, C. Y., 2007, "Testing Process Precision for Truncated Normal Distributions," Microelectron. Reliab., **47**(12), pp. 2275–2281.
[2] Li, M. H. C., 2004, "Optimal Target Selection for Unbalanced Tolerance Design," Int. J. Adv. Manuf. Technol., **23**(9–10), pp. 743–749.
[3] Pearn, W. L., Lin, P. C., Chang, Y. C., and Wu, C. W., 2006, "Quality Yield Measure for Processes With Asymmetric Tolerances," IIE Trans., **38**(8), pp. 619–633.
[4] Karamanis, D., 2011, "Management of Moderate Wind Energy Coastal Resources," Energy Convers. Manage., **52**(7), pp. 2623–2628.
[5] Xie, K., and Billinton, R., 2011, "Energy and Reliability Benefits of Wind Energy Conversion Systems," Renewable Energy, **36**(7), pp. 1983–1988.
[6] Anyi, M., and Kirke, B., 2010, "Evaluation of Small Axial Flow Hydrokinetic Turbines for Remote Communities," Energy Sustainable Dev., **14**(2), pp. 110–116.
[7] Agarwal, P., and Manuel, L., 2009, "Simulation of Offshore Wind Turbine Response for Long-Term Extreme Load Prediction," Eng. Struct., **31**(10), pp. 2236–2246.
[8] Ronold, K. O., and Larsen, G. C., 2000, "Reliability-Based Design of Wind-Turbine Rotor Blades Against Failure in Ultimate Loading," Eng. Struct., **22**(6), pp. 565–574.

Downloaded From: http://mechanicaldesign.asmedigitalcollection.asme.org/ on 03/21/2013 Terms of Use: http://asme.org/terms

[9] Carpinteri, A., Ferro, G., and Invernizzi, S., 1997, "The Nominal Tensile Strength of Disordered Materials: A Statistical Fracture Mechanics Approach," Eng. Fract. Mech., **58**(5–6), pp. 421–435.
[10] Sia, A. H. I., and Dixon, N., 2007, "Distribution and Variability of Interface Shear Strength and Derived Parameters," Geotextiles and Geomembranes, **25**(3), pp. 139–154.
[11] Deperrois, A., Bignonnet, A., and Merrien, P., "Probabilistic Design Methods for Multiaxial High-Cycle Fatigue," 1996, *Multiaxial Fatigue and Design: Papers Presented at the Fourth International Conference on Biaxial/Multiaxial Fatigue*, A. Pineau, A, Cailletaud, and T. C. Lindley, eds., Saint-Germainen Laye, France, Mechanical Engineering Publications, London, p. 445–460.
[12] Verrill, S., and Kretschmann, D. E., 2009, "Material Variability and Repetitive Member Factors for the Allowable Properties of Engineered Wood Products," J. Test. Eval., **37**(6), pp. 607–615.
[13] Beauval, C., and Scotti, O., 2004, "Quantifying Sensitivities of Psha for France to Earthquake Catalog Uncertainties, Truncation of Ground-Motion Variability, and Magnitude Limits," Bull. Seismol. Soc. Am., **94**(5), pp. 1579–1594.
[14] Beauval, C., Hainzl, S., and Scherbaum, F., 2006, "Probabilistic Seismic Hazard Estimation in Low-Seismicity Regions Considering Non-Poissonian Seismic Occurrence," Geophys. J. Int., **164**(3), pp. 543–550.
[15] Beauval, C., Honoré, L., and Courboulex, F., 2009, "Ground-Motion Variability and Implementation of a Probabilistic-Deterministic Hazard Method," Bull. Seismol. Soc. Am., **99**(5), pp. 2992–3002.
[16] Du, X., 2008, "Unified Uncertainty Analysis by the First Order Reliability Method," J. Mech. Des., **130**(9), pp. 091401–091410.
[17] Zhao, Y.-G., and Ono, T., 1999, "General Procedure for First/Second-Order Reliability Method (Form/Sorm)," Struct. Safety, **21**(2), pp. 95–112.
[18] Guo, J., and Du, X., 2010, "Reliability Analysis for Multidisciplinary Systems With Random and Interval Variables," AIAA J., **48**(1), pp. 82–91.
[19] Awad, M., Singh, N., and Sudjianto, A., 2006, "Mpp Search Method Using Limited Radial Importance Sampling," Int. J. Prod. Dev., **3**(3–4), pp. 305–318.
[20] Du, X., and Sudjianto, A., 2003, "Reliability-Based Design with the Mixture of Random and Interval Variables," J. Mech. Des., **127**(6), pp. 1068–1077.
[21] Huang, H. Z., Yu, H., Zhang, X., Zeng, S., and Wang, Z., 2010, "Collaborative Optimization with Inverse Reliability for Multidisciplinary Systems Uncertainty Analysis," Eng. Optimiz., **42**(8), pp. 763–773.
[22] Lee, I., Choi, K. K., Du, L., and Gorsich, D., 2008, "Inverse Analysis Method Using Mpp-Based Dimension Reduction for Reliability-Based Design Optimization of Nonlinear and Multi-Dimensional Systems," Comput. Methods Appl. Mech. Eng., **198**(1), pp. 14–27.
[23] Lee, I., Choi, K. K., and Gorsich, D., 2010, "System Reliability-Based Design Optimization Using the Mpp-Based Dimension Reduction Method," Struct. Multidiscip. Optim., **41**(6), pp. 823–839.
[24] Zhang, J., and Du, X., 2010, "A Second-Order Reliability Method With First-Order Efficiency," Trans. ASME, J. Mech. Des., **132**(10), pp. 101006–101014.
[25] Melchers, R. E., Ahammed, M., and Middleton, C., 2003, "Form for Discontinuous and Truncated Probability Density Functions," Struct. Safety, **25**(3), pp. 305–313.
[26] Millwater, H., and Feng, Y., 2011, "Probabilistic Sensitivity Analysis With Respect to Bounds of Truncated Distributions," Trans. ASME J. Mech. Des. **133**(6), pp. 061001–091011.
[27] Zhang, T., and Xie, M., 2011, "On the Upper Truncated Weibull Distribution and Its Reliability Implications," Reliab. Eng. Syst. Saf., **96**(1), pp. 194–200.
[28] Raschke, M., 2011, "Inference for the Truncated Exponential Distribution," Stochastic Environmen. Res. Risk Assess., pp. 1–12.
[29] Griffin, D. W. K., 2002, "Aircraft Structural Design Geared for High Reliance on Analysis for Acceptance," Paper presented at the RTO A VT Symposium on "Reduction of Military Vehicle Acquisition Time and Cost through Advanced Modelling and Virtual Simulation held in Paris, France, April 22–25, Report No. RTO-MP-089, pp. 25.1–25.19.
[30] Butler, R. W., and Wood, A. T. A., 2004, "Saddlepoint Approximation for Moment Generating Functions of Truncated Random Variables," Ann. Stat., **32**(6), pp. 2712–2730.
[31] Emancipator, K., and Kroll, M. H., 1993, "A Quantitative Measure of Nonlinearity," Clin. Chem., **39**(5), pp. 766–772.
[32] Butler, R. W., 2007, *Saddlepoint Approximations with Applications, Cambridge Series in Statistical and Probabilistic Mathematics*, Cambridge University, Cambridge.
[33] Butler, R. W., Sutton, R. K., Booth, J. G., and Strickland, P. O., 2008, "Simulation-Assisted Saddlepoint Approximation," J. Statist. Comput. Simul., **78**(8), pp. 731–745.
[34] Daniels, H., 1954, "Saddlepoint Approximations in Statistics," Ann. Math. Stat., **25**(4), pp. 631–650.
[35] Du, X., 2010, "System Reliability Analysis With Saddlepoint Approximation," Struct. Multidiscip. Optim., **42**(2), pp. 193–208.
[36] Du, X., and Sudjianto, A., 2004, "A Saddlepoint Approximation Method for Uncertainty Analysis," ASME 2004 International Design Engineering Technical Conferences, ASME, Salt Lake City, UT, Vol. 1, pp. 445–452.
[37] Jensen, J. L., 1995, *Saddlepoint Approximations, Oxford Statistical Science Series*, Clarendon, Oxford, Vol. 16.
[38] Du, X., and Sudjianto, A., 2004, "First-Order Saddlepoint Approximation for Reliability Analysis," AIAA J., **42**(6), pp. 1199–1207.
[39] Huang, B., and Du, X., 2006, "Uncertainty Analysis by Dimension Reduction Integration and Saddlepoint Approximations," Trans. ASME J. Mech. Des., **128**(1), pp. 26–33.
[40] Huang, B., and Du, X., 2008, "Probabilistic Uncertainty Analysis by Mean-Value First Order Saddlepoint Approximation," Reliab. Eng. Syst. Saf., **93**(2), pp. 325–336.
[41] Renshaw, E., 2000, "Applying the Saddlepoint Approximation to Bivariate Stochastic Processes," Math. Biosci., **168**(1), pp. 57–75.
[42] Lugannani, R., and Rice, S. O., 1980, "Saddle Point Approximation for the Distribution of the Sum of Independent Random Variables," Ann. Appl. Probab., **12**(2), pp. 475–490.

Downloaded From: http://mechanicaldesign.asmedigitalcollection.asme.org/ on 03/21/2013 Terms of Use: http://asme.org/terms